http://dx.doi.org/10.21611/qirt.2012.294

QIRT 2012

11th International Conference on
Quantitative InfraRed Thermography

# Infrared cameras in airborne remote sensing: IR-Imagery for photogrammetric processing at German Aerospace Center DLR, Berlin

by S. Pless*, B. Vollheim**, M. Haag* and G. Dammaß**

* German Aerospace Center DLR, Institute of Optical Information Systems, Rutherfordstr. 2, 12489 Berlin, Germany, *sebastian.pless@dlr.de*

**InfraTec GmbH, Gostritzer Str. 61- 63, 01217 Dresden, Germany, *b.vollheim@infratec.de*

**Abstract**

This article describes the use of infrared cameras for aerial imaging and the processing of generated data into thermal orthophotos. For this task two cameras with cooled infrared detectors have been tested: The InfraTec ImageIR 8300 (InSb) and 8800 (MCT) for the mid-wave and long-wave infrared range, respectively. The prerequisite for a photogrammetric processing of the images is the exact radiometric and geometric calibration of the cameras. Also, the camera setup and the modifications necessary for the flight campaign are described. The results of this project are a thermal orthophoto and a digital surface model generated from the thermal images.

## 1. Introduction

Thermal mapping applications are becoming more important, as energy losses by heat dissipation are undesirable from both an economical and an ecologic point of view. For high-resolution mapping and for deriving specialized products from aerial thermal imagery, high accuracy photogrammetric processing is necessary.

At the Institute of Optical Information Systems of the German Aerospace Center, airborne and spaceborne camera systems are tested, developed and used. Furthermore, methods for processing the data from such camera systems for various applications are developed and refined.

The combination of a suitable thermographic camera system, subsystems for acquiring aerial image data and methods for processing this data leads to a new class of thermal imaging products, including 3D data.

## 2. Camera system

In this section the camera components involved in the project will be introduced. Special emphasis will be put on camera calibration, as this is key for deriving high accuracy photogrammetric products. In addition, radiometric calibration is essential for the quantification of temperature variations over a scene.

### 2.1 General Camera Configuration

Thermographic cameras used for airborne remote sensing must provide a high thermal and geometrical resolution as well as a very fast response. These demands are fulfilled by infrared cameras with cooled Focal Plane Array (FPA) detectors. The arrays are usually composed of infrared photodiodes or Quantum Well Infrared Photodetectors (QWIP) which have to be cooled to cryogenic temperatures to reduce the dark current. These so-called photon or quantum detectors react immediately on a changing infrared radiation level with response times on the order of 1 µs. The image capturing of state-of-the-art cooled FPA detectors occurs according to the global shutter (or snapshot) principle by integrating the photo signals of all pixels at the same time.

Cameras with uncooled microbolometer detectors are less suitable for airborne imaging even though their thermal and geometrical resolution has been considerably improved over the past years. The inherent high time constants (4 … 10 ms) of these thermal detectors [1] and the row-by-row read-out comparable to a rolling shutter principle lead to a smearing of the acquired images during a flight.

The described flight campaigns were carried out with cameras from the series ImageIR manufactured by InfraTec GmbH, Germany [2]. This high-end camera series covers various cooled detector types with different photodiode materials - indium antimonide (InSb) or mercury cadmium telluride (MCT) - for both the mid-wave infrared (MWIR) and long-wave infrared (LWIR) range as well as several FPA dimensions from 320 x 256 to 1280 x 1024 pixels. The used camera types were an ImageIR 8300 equipped with a 640 x 512 MWIR InSb detector and an ImageIR 8800 with a 640 x 512 MCT detector for the LWIR spectral range.

Figure 1 shows a camera head of the ImageIR series. The camera housing can easily be mounted in different carrier systems without extensive additional efforts and is suited for a usage even under harsh ambient conditions. The camera electronics supports the data acquisition in both continuous and triggered modes which are also essential requirements for airborne imaging.

http://dx.doi.org/10.21611/qirt.2012.294


***Fig. 1.*** *High-resolution thermographic camera ImageIR 8300 by InfraTec*

**2.2 Camera design**

The camera series ImageIR was designed on a modular principle to allow an inexpensive adaptation of different cooled detectors and various lenses. The camera housing consists of three separate modules. The front module contains the lens interface and the opto-mechanical assemblies like filter or aperture wheel. The central detector module includes the detector with the associated proximity electronics, an image processing and controller unit and the internal power supply. High-precision fits ensure low mechanical tolerances between front and detector module. The interface module contains the output interfaces and provides all external connectors at the backside of the camera housing. The common camera outputs are Gigabit-Ethernet (GigE) or CameraLink.

State-of-the-art detectors are equipped with an integrated cryogenic cooler operating according to the Stirling principle. FPA and cooler are already joined by the detector manufacturer in a compact Integrated Detector Cooler Assembly (IDCA). The main challenge for the camera design is the efficient heat dissipation from the warm side of the Stirling cooler to the environment. This requires a low thermal resistance of the housing without neglecting the degree of protection against dust and humidity. Furthermore, the air temperature inside the detector module which influences not only the power consumption but also the lifetime of the cooler must be reduced as far as possible by minimizing the power loss of the camera electronics. The front module of the housing is widely thermally isolated from the detector module to ensure a sufficient temperature stability in the optical channel between detector and lens. By these means, the camera can be operated in a wide ambient temperature range between –20 and 50°C without a degradation of the image quality and the measuring accuracy.

**2.3 Radiometric calibration**

IR detector arrays exhibit a considerably worse response uniformity than detectors for the visible spectral range. The detector output signals must undergo a Non-Uniformity-Correction (NUC) to achieve an acceptable image quality. For MWIR photodiode arrays it is usually sufficient to correct the gain and the offset of each pixel. For this, two homogeneous images at different signal levels, i.e. radiation temperatures, are detected and processed to estimate two correction coefficients per pixel. This procedure is commonly called 2-point NUC.

The success of a 2-point NUC depends primarily on the linearity of the photodiodes. For nonlinear power/signal characteristics, the remaining deviation of the pixel signals after correction – called Remaining Fixed Pattern Noise (RFPN) – is too large to provide a satisfying image quality over a wide signal range [3]. This is the case for the most high-resolution LWIR MCT photodiode arrays. As the internal resistance of MCT diodes decreases considerably with an increasing cut-off wavelength, LWIR MCT photodiodes have a much higher and more differing dark current than MWIR MCT photodiodes [4]. Therefore, the offset span of a LWIR MCT FPA is much larger which reduces the remaining dynamic range for the photo signals. The offsets of InSb and MCT photodiode arrays for the MWIR spectral range are comparable. The offset range of an MWIR InSb and an LWIR MCT detector, both with 640 x 512 pixels and similar response, are compared in figure 2.

http://dx.doi.org/10.21611/qirt.2012.294


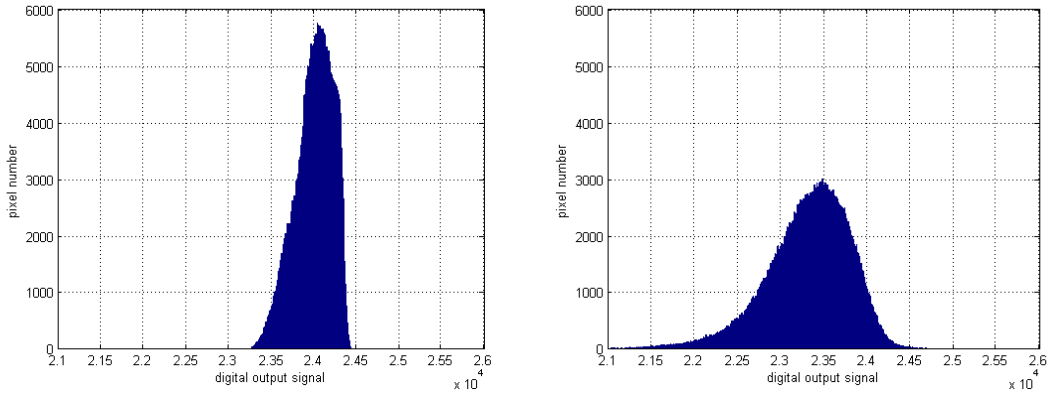


***Fig. 2.*** *Statistical signal distribution of an MWIR InSb FPA (left) and an LWIR MCT FPA (right) with 640 x 512 pixels for 23°C object temperature*

The power/signal characteristic of the single LWIR MCT photodiodes shows a higher nonlinearity than MWIR photodiodes, which requires the introduction of a third nonlinear term in the correction formula. This correction is usually called 3-point NUC since three homogeneous images at different signal levels are required to calculate three correction coefficients per pixel. Figure 3 shows the signal/temperature curves of a typical 640 x 512 LWIR MCT photodiode array after eliminating the non-operating or 'bad' pixels. The results of both a 2-point and a 3-point NUC are compared for this set of curves in figure 4. The best homogeneity is reached at the NUC points whereas the remaining deviation – the RFPN – increases between and beyond, respectively, these points. The signal levels for the NUC must be chosen in such a way that the remaining deviations are minimized over the whole interesting temperature range. Figure 4 shows that the RFPN of a LWIR MCT photodiode array can be significantly reduced by applying a 3-point NUC.

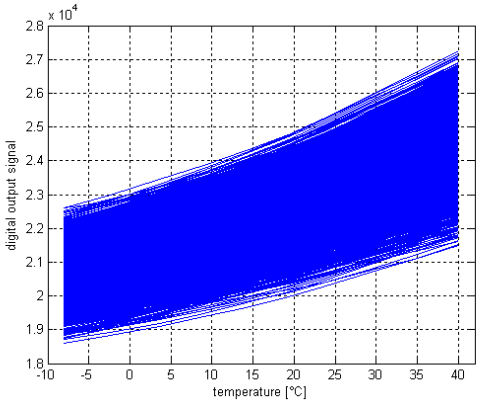


***Fig. 3.*** *Signal/temperature curves of a 640 x 512 LWIR MCT photodiode array (without bad pixels)*

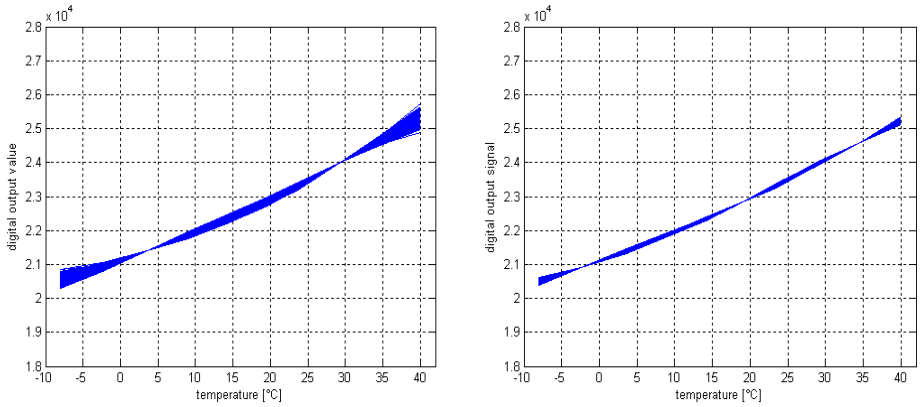


***Fig. 4.*** *Signal/temperature curves (of figure 3) after 2-point NUC (left) and 3-point NUC (right)*

The correction coefficients of MWIR photodiode arrays are sufficiently long-term stable so that only a slight offset adjustment is recommended before starting an operating session [5]. The NUC tables of LWIR MCT arrays are, however, only valid for some hours. They must especially be refreshed after each cooldown of the IDCA. An additional offset adjustment improves the image quality only for a small signal range. The execution of such a 3-point NUC by means of homogeneous radiation sources could be carried out in laboratories but wouldn't be acceptable for practical applications like aerial imaging. To allow a frequent 3-point NUC without external radiation sources, an internal temperature-controlled blackbody was implemented in the front module of LWIR cameras. This internal blackbody is realized by a Peltier element which is mounted on a motorized wheel. This solution ensures reproducible and stable NUC results for all ambient conditions. Figure 5 demonstrates the improvement of the image quality by performing an internal 3-point NUC after a cooldown.

***Fig. 5.*** *Thermal images of an LWIR MCT camera after cooldown, before (left) and after (right) an internal NUC*

In comparison to so-called thermal imagers a thermographic camera is not only able to detect a thermal image but also to estimate the surface temperature of the observed objects. The relation between object temperature and (corrected) camera output signal is determined by a radiometric calibration. The defined object temperatures are provided by so-called blackbodies – these are radiation sources which behave nearly as ideal thermal radiators. The real temperatures of the involved blackbodies are monitored by high-precision calibrated reference pyrometers. The measured temperature/signal pairs are transferred into a response curve f=signal(temperature). These response curves are estimated at different ambient temperatures to gain input parameters for a subsequently applied drift compensation algorithm.

The response of a thermographic camera can be adjusted to the requirements of the special application by changing the integration time for the photodiode current or by means of apertures or optical filters. The upper temperature of a measuring range is limited by the dynamic range. The lower temperature is defined by the minimum required response. The complete response curves don't cover the full dynamic range of the detector as the signal offsets between the pixels occupy a part of this range. A smaller part of the dynamic range must be reserved for the ambient temperature induced signal drift. The cameras of the ImageIR series provide a dynamic range of 14 bit.

### 2.4 Geometric calibration

For photogrammetric processing a corrected image following the pinhole camera model is needed. While the size of the detector is known in sufficient accuracy, the focal length of the optics, the position of the principal axis in relation to the detector and the parameters of the distortion have to be measured. For this project a 25 mm lens was used together with the ImageIR 8300.

For this task a setup consisting of a thermal infrared collimator and a two axis positionable manipulator table (gimbal) was used. The camera is positioned on the gimbal with the entrance pupil roughly in the rotation center of both axis to ensure a view on the collimator ray from a wide variety of angles. The thermal infrared collimator is fixed in relation to the gimbal (figure 6).

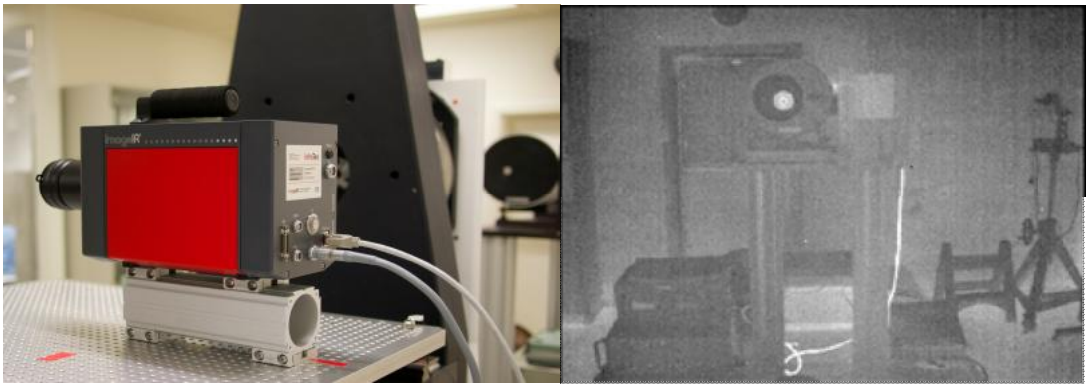

***Fig. 6.*** *Left: ImageIR 8300 mounted on manipulator table, thermal infrared collimator in the background. Right: View of the collimator from camera (amplified contrast for visualization)*

The manipulator now is moved to an array of angles. For the geometric calibration of the ImageIR 8300 (with 25 mm lens) 48 measurements have been taken. The accuracy of the manipulator table is higher than 3 x $10^{-3}$ degrees of arc.

For each angle the collimator ray is recorded in a thermal image. The collimator target is selected according to the focal lengths of collimator and camera lens to ensure a useful projection size on the camera detector. The subpixel position of the collimator ray projection on the detector is determined by using Gaussian fit algorithms.

Focal length, principal axis and lens distortion are determined from this information using the camera model described in [6]. A visualization of the measured and corrected positions is given in figure 7.

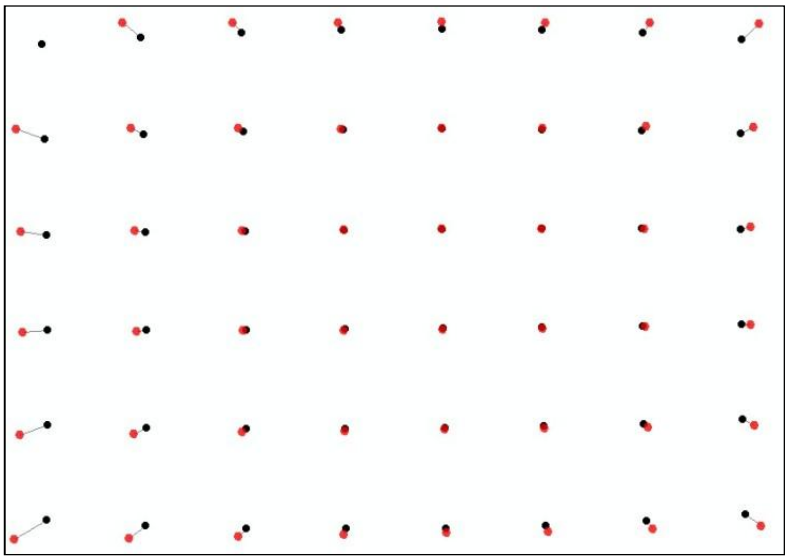

***Fig. 7.*** *Measured positions of the collimator ray (black) and corrected projections after distortion correction (red)*

## 3. Data acquisition

The site of the German Aerospace Center in Berlin Adlershof is used as a test field for different flight campaigns using a wide variety of sensor systems ranging from standard cameras recording visible light to LIDAR systems and hyper spectral scanners. For this task a set of about 500 ground control points has been built up and is constantly kept up-to-date. Additionally, data sets from the different sensor systems are stored for comparison.

Albeit the ground control points are mostly not suitable for referencing thermal imagery, this test site was used for testing the ImageIR 8300 thermographic camera.

### 3.1 Hardware setup

The setup inside the aircraft was similar to an aerial camera setup for photogrammetric data acquisition. Figure 8 shows the acquisition setup inside the Rockwell AeroCommander AC640 used.

The thermographic camera was mounted on a Somag GSM 3000 stabilization platform. Because of the comparatively low pixel count of infrared cameras it is essential to use stabilization. If the camera looked off-nadir due to aircraft movements, resolution would become uneven across the surveyed area, overlap would change and photogrammetric processing would become more difficult.

The movements of the camera were recorded by a combined global positioning and inertial navigation system (IGI AeroControl with IMU IId 256 Hz). The trigger output of the camera was connected to the event input of the GPS/INS. For each recorded image a GPS time stamp was recorded and position and attitude of the camera could be assigned to each thermal image afterwards.

Data acquisition was controlled and monitored by a laptop computer using the IRBIS® vision software supplied by InfraTec. Additionally, hardware from the Modular Airborne Camera System project [10] was used for data handling and power distribution.

***Fig. 8.*** *Setup inside aircraft during data acquisition. ImageIR 8300 mounted lens down on stabilization platform, IMU mounted next to camera, auxiliary hardware inside rack, laptop showing actual thermal images*

### 3.2 Flight campaign

The terms for planning and executing a flight campaign with a thermographic camera are comparable to a campaign with a standard airborne camera system, although some alterations have to be considered.

The most remarkable difference is the ideal time frame. Direct sunlight should be avoided to minimize temperature variations in homogenous areas caused by shadowing effects. To minimize temperature changes while data acquisition the campaign should be carried out around the turning point of the diurnal temperature variations. Therefore, the best time for a thermal flight is at night, ideally around the time when ambient temperatures are lowest. This also helps to detect energy losses, as the difference to temperatures of heated objects is maximized.

In order to provide well-recognisable ground control points, several heat-emitting devices were placed inside the target area. The coordinates of these points were surveyed with a precision higher than 5 cm using differential GPS. Also, temperature measurements of different materials were recorded at ground level throughout the campaign, in order to access the accuracy of the measured temperatures of the aerial images.

The altitude of the flight was 730 m above ground, resulting in a ground resolution of 0.8 m per pixel. The flight lines were planned for the images to have an overlap of 60% between the image stripes (see figure 9). The camera was operated with a frame rate of 10 Hz, so the overlap between single images in flight direction was as high as 98%.

http://dx.doi.org/10.21611/qirt.2012.294


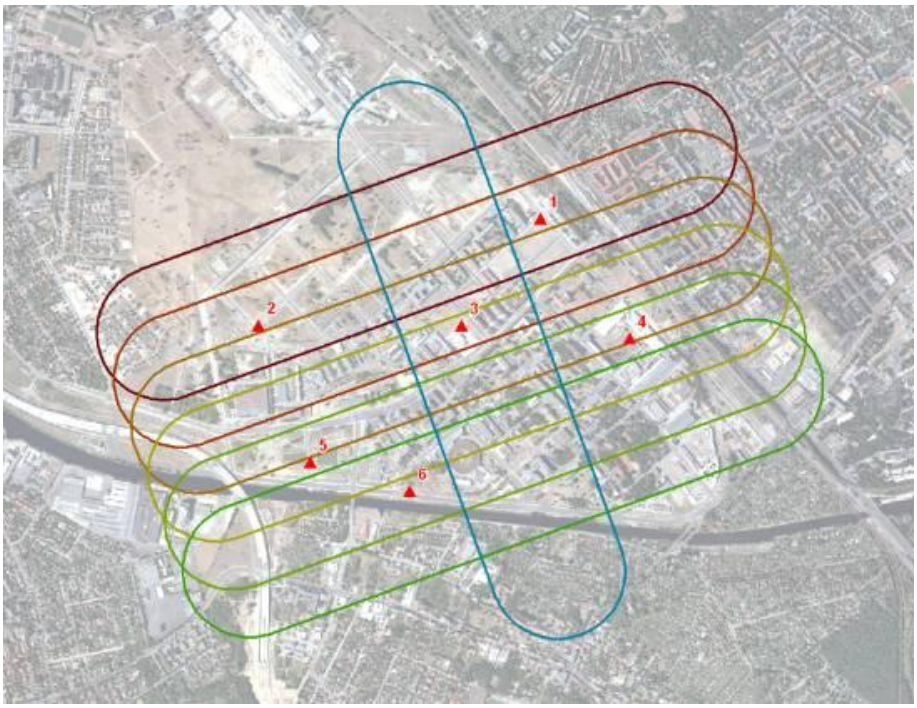


***Fig. 9.*** *Flight planning showing the extent of the image stripes (multicolor) and the position of the heat-emitting ground control points (red triangles)*

Due to air traffic safety restrictions the flight had to be carried out earlier than planned. Acquisition started at 0:50 a.m. local time and ended at 1:25 a.m. local time (CEST). Ground speed of the aircraft for the measurements was 220 kn (~400 km/h). 3911 thermal images have been recorded in total for this campaign.

## 4. Photogrammetric processing

### 4.1 Preprocessing

The thermographic camera provides image data in real-time to a host computer by means of a GigE interface. The digital data (14 bit) which include all radiometric information are stored in a special file format named 'IRB'. Additional information like camera temperature, lens type or GPS can also be stored within the IRB files. Various software tools for remote control, data acquisition and analyses as well as a software development kit are available. The frame-sync trigger output of the camera can be used to synchronize each image with GPS. Single image data or image sequences can be exported into various standard formats like XLS, ASCII, TIF, BMP or AVI.

For this project, image data was exported to TIF. This was necessary to apply the geometric corrections described in 2.4 and for further photogrammetric processing.

GPS data was corrected using GPS measurements, delivered in Receiver Independent Exchange Format (RINEX) from a reference station near the target area. Lever arms from sensor to inertial measurement unit (IMU) and GPS antenna also have been measured and incorporated. Position and attitude information for each image with an accuracy as described in [7] has been created and assigned to the images.

While the direct georeferencing from GPS/INS data is sufficient for generating a thermal orthoimage and even a surface model with reduced resolution, an aerotriangulation has been carried out using INPHO software (figure 10). The coordinates from thermal ground control points have been used to improve absolute position accuracy [8].

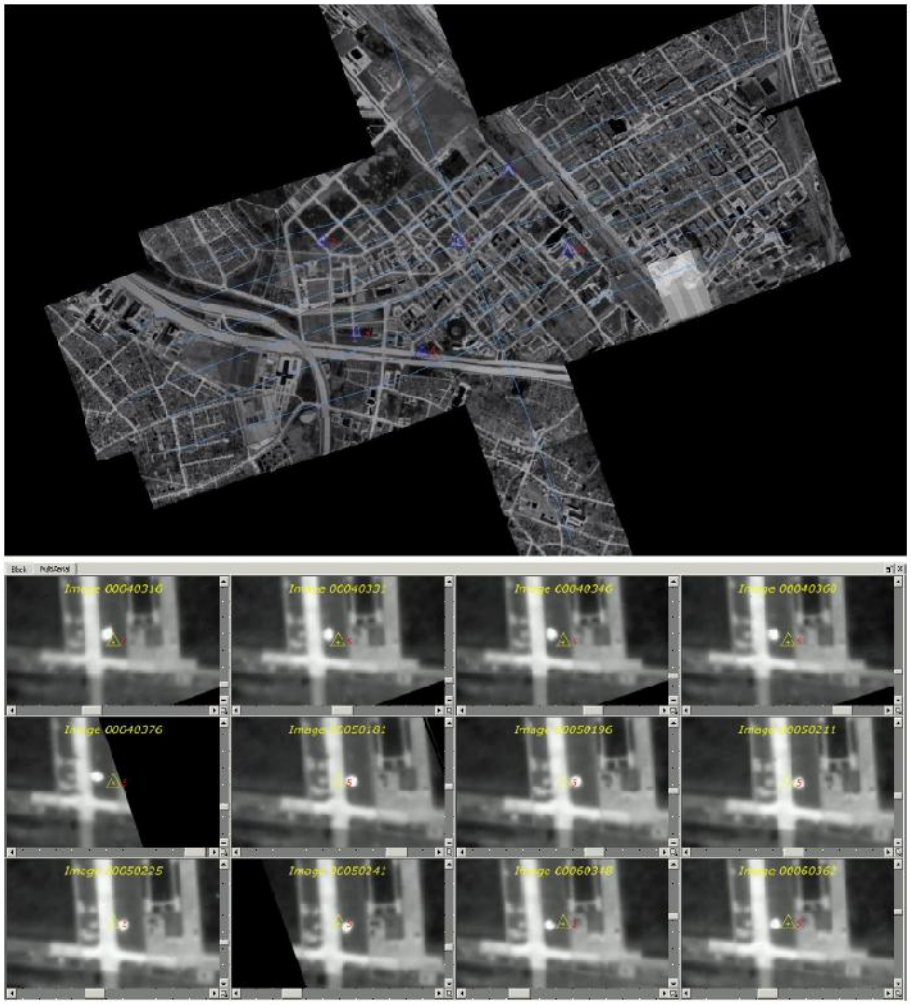

***Fig. 10.*** *Orientation of the thermal images in INPHO*

### 4.2 Digital Surface Model and orthoimage generation

From the oriented images a digital surface model was derived using the internal matching algorithms. This model has a reduced resolution of 6 m in planimetry and 1 m in height. By projecting the images onto this model a thermal orthoimage with 80 cm resolution has been generated. Figure 11 shows a subset of this data product. The thermal information is coded in greyscales values from colder temperatures (lower pixel values, darker image areas) to warmer regions (higher pixel values, brighter image areas). Ground control points were used for verification of the accuracy of the orthoimage, results are shown in table 1.

***Table 1.*** *Accuracy of ground control points*

| Point | Deviation X [m] | Deviation Y [m] |
|---|---|---|
| 1 | -0.14 | 0.04 |
| 2 | -0.9 | 0.08 |
| 3 | -0.13 | -0.03 |
| 4 | -0.03 | 0.05 |
| 5 | -0.12 | 0.24 |
| 6 | 0.102 | -0.05 |
| RMS | 0.353 | 0.103 |

***Fig. 11.*** *Thermal orthoimage derived from ImageIR 8300 data*

The quality of the image orientation allowed for the use of another matching algorithm, developed by H. Hirschmüller at the DLR Institute of Robotics and Mechatronics, the Semi-Global Matching [9]. This algorithm generates a height value for each ground pixel. The result is a full resolution surface model (80 cm in planimetry and 50 cm in height). A comparison of both surface models is shown in figure 12.

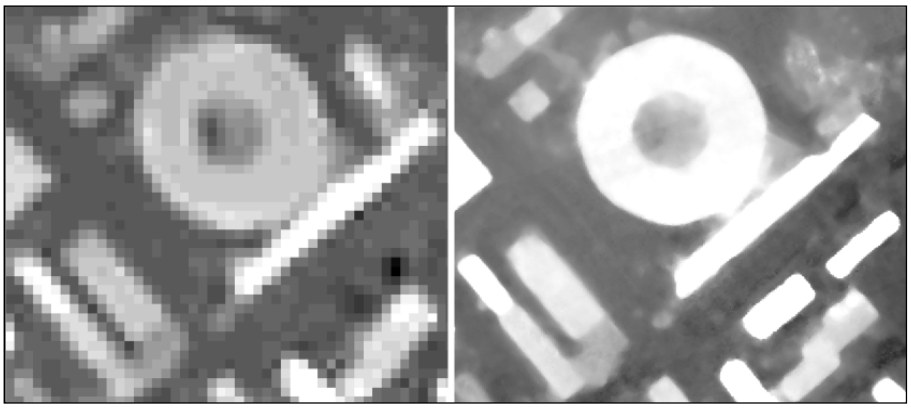

***Fig. 12.*** *Digital surface model generated from thermal imagery. Left: INPHO model, 6 m GSD, right: SGM model, 80 cm GSD*

By projecting the images on the high resolution Digital Surface Model a True Orthoimage is generated. As each pixel has its own height value, position errors due to different viewing angles, occlusion and other surface model related effects are eliminated. The images are map projected and can be used for accurate measurements.

By combining the high resolution Digital Surface Model with the thermal infrared True Orthoimage, an interactive 3D model can be generated (figure 13).

***Fig. 13.*** *3D model from combination of DSM and True Orthoimage*

For the data acquisition the Image IR 8300 thermographic camera was set to an emissivity value of ε=1. As there are a lot of different materials in the observed scene, this will lead to false temperature readings for all surfaces, to be strict. This could only be rectified with a classification of surfaces and the inclusion of correction coefficients.

In the vicinity of one ground control point temperature measurements for three different surfaces were taken during the campaign. For these measurements a handheld infrared thermometer Optris LS was used. For comparison it was also set to ε=1. The results of the comparison in table 2 indicate an intact radiometric response from the photogrammetric data products. As the control surfaces are covered by several pixels, a range rather than a single number is specified for the airborne values.

***Table 2:*** *Comparison of temperatures from ground measurements and aerial data.*

| Material | Ground measurement | Orthoimage temperature |
|---|---|---|
| Area 1 (asphalt) | 17.24 °C | 17.3 … 17.6 °C |
| Area 2 (concrete) | 15.77 °C | 15.3 .. 15.8 °C |
| Area 3 (sand) | 11.27 °C | 10.9 .. 11.8 °C |

## 5. Conclusion and outlook

Photogrammetric processing of aerial thermal images is possible if the thermographic camera is qualified and distinct parameters are controlled. The use of a 'global shutter' or 'snapshot' detector with the ability to generate a trigger signal when exposing an image is one of these essential qualifications.

While geometric calibration is required for the generation of photogrammetric products like Digital Surface Models, True Orthoimages and 3D models, radiometric calibration is needed for exact temperature measurements. The project described in this paper indicates that radiometric calibration can be held intact throughout photogrammetric processing.

The tests have shown that the InfraTec ImageIR cameras are suitable for generating high quality airborne photogrammetric products due to an appropriate radiometric calibration and a stable geometry. The described method for geometric calibration is time-consuming and requires special equipment, different methods should be evaluated.

To extend the usefulness of the data products further developments in photogrammetric processing are currently developed. While the camera also detects façade information none of this is used in the final products for now. A complete thermal 3D model showing the complete envelope of buildings will open great opportunities for airborne use of thermographic cameras.

## REFERENCES

[1] Yon J.-J., et. al., "Latest amorphous silicon microbolometer developments at LETI-LIR", Infrared Technology and Applications XXXIV, Proc. of SPIE Vol. 6940, pp. 69401W 1-8, Orlando 2008.
[2] InfraTec GmbH, "High-end Camera Series ImageIR®", Datasheet, Dresden 2012.
[3] Wang R., et. al., "An improved nonuniformity correction algorithm for infrared focal plane arrays which is easy to implement", Infrared Physics & Technology, Vol. 39, pp. 15-21, 1998.
[4] Destefanis G. L., et. al., "Recent developments in infrared detectors at LIR", 3rd Int. Conf. on Advanced Infrared Detectors and Systems", Proc. of IEE, pp. 44-49, London 1986.
[5] Combette A., et.al., "Non-uniformity correction results for SOFRADIR infrared 2D staring arrays", Infrared Technology and Applications XXXIII, Proc. of SPIE Vol. 6542, pp. 65423Q, Orlando 2007.
[6] Bauer, M., Griessbach, D., Hermerschmidt, A., Krüger, S., Scheele, M. & Schichmanow, A., "Geometrical camera calibration with diffractive optical elements", Optics Express, Vol. 16, Issue 25, pp. 20241-20248, Sydney 2008.
[7] Scholten, F., Sujew, S., Gwinner, K., "Application of GPS/INS-Systems with the HRSC - A Comparison of APPLANIX POS/AV-510 and IGI AEROcontrol-IId." In: Proceedings of the ISPRS Workshop Working Group i/5 Theory, Technology and Realities of Inertial/GPS Sensor Orientation, 22nd and 23rd of September 2003, Castelldefels, Spain 2003.
[8] Haag, M., "Photogrammetrische Auswertung von Bilddaten eines thermalen Sensors", master thesis, Beuth University of Applied Sciences, Berlin 2010.
[9] Hirschmüller, H., "Stereo Processing by Semiglobal Matching and Mutual Information. ", IEEE Transactions on pattern analysis and machine intelligence, Vol. 30, No. 2, 2008.
[10] Lehmann, F., Berger, R., Brauchle, J., Hein, D., Meißner, H., Pless, S., Strackenbrock, B. "MACS - Modular Airborne Camera System for generating photogrammetric high-resolution products." Photogrammetrie Fernerkundung Geoinformation, 2011 (6), pp. 435-446. E. Schweizerbart'sche Verlagsbuchhandlung, Stuttgart 2011.